PHYSICAL REVIEW B VOLUME 52, NUMBER 20 15 NOVEMBER 1995-II

Ab initio calculation of phonon spectra for graphite, BN, and BC_2N sheets

Yoshiyuki Miyamoto,* Marvin L. Cohen, and Steven G. Louie
Department of Physics, University of California at Berkeley, Berkeley, California 94720-7300
and Materials Sciences Division, Lawrence Berkeley Laboratory, Berkeley, California 94720

(Received 7 June 1995)

Phonon spectra for graphitic sheets of carbon, BN, and BC_2N are computed and studied. The dynamical matrices are constructed from force constants obtained by performing supercell Hellmann-Feynman force calculations within the framework of the local-density approximation. The calculated phonon dispersions of the BC_2N sheet are found to be similar to a superposition of those of graphite and BN sheets. Geometrical relations between the calculated phonon modes of the BC_2N sheet and those of graphite and BN sheets are discussed.

I. INTRODUCTION

Graphitic sheet structures are found not only for carbon but also for compounds such as BN, BC_3,[1] and BC_2N.[2] The electronic structures of these graphitic compounds have been investigated using first-principles calculations.[3–5] Despite a common honeycomb pattern in atomic arrangement, the calculated electronic structures of these compounds show different properties. Because of the C substitution by B atoms, the BC_3 sheet has both π and π^* bands above the Fermi level in the proposed atomic geometry.[4] The calculated electronic density of states is consistent with the electron energy loss spectroscopy data.[1] The most stable atomic structure of the BC_2N sheet was theoretically predicted[5] to have zigzag chains of C-C and B-N atoms. This structure results in an anisotropic electron energy band structure. Tubule forms of these compounds were proposed[6,7] to be as likely to form as carbon nanotubes which were known to exist,[8] and recently nanotubes originating from graphitic compounds of $B_xC_yN_z$ have been synthesized.[9] According to first-principles and tight-binding calculations,[6,7] the electronic properties of the sheets formed from $B_xC_yN_z$ should be retained in the tubule forms. Hence, knowledge of the electronic structures of graphitic sheets are important and useful to understand the electronic structures of their tubule forms.[10]

Beside the electronic structures, theoretical and experimental information about phonon properties is also useful to characterize these graphitic compounds as are investigations of electron-phonon interactions which play crucial roles in normal and superconducting transport properties. Phonons of graphite are well investigated both experimentally[11] and theoretically,[12] and the electron-phonon couplings have been studied for graphite sheets[13] and carbon nanotubes.[14] However, details related to phonon dispersions and vibrational modes of the B-C-N compounds have not been reported to our knowledge.

In this paper, we focus on the relations between phonons in graphite, BN, and BC_2N sheets. For the BC_2N sheet, the most stable structure[5] shown in Fig. 1 can be interpreted as a mixture of graphite and BN sheets. Hence the phonon modes of the BC_2N sheet are expected to be related to those of graphite and BN sheets. We have performed calculations for the phonon spectra of graphite, BN, and BC_2N sheets within the harmonic approximation. The calculated phonon frequencies of the BC_2N sheet are found to be similar to a superposition of those of graphite and BN sheets. The major features of the phonon modes for the BC_2N sheet have similarities to those of graphite and BN sheets at most wave vectors in the Brillouin zone (BZ), but show a sharp contrast along a particular line of wave vectors. In the rest of this paper, we present the details of our calculations and discussion.

II. CALCULATION

Within the harmonic approximation, the phonon frequencies and polarizations are obtained by diagonalizing the dynamical matrices given at each wave vector $\mathbf{k}$ by

$$D^{\mathbf{i},\mathbf{j}}_{\alpha,\beta}(\mathbf{k}) = \frac{1}{\sqrt{\mathbf{M_i M_j}}} \sum_{\mathbf{R}} \exp\{i\mathbf{k}\cdot(\tau_{\mathbf{i}} - \tau_{\mathbf{j}} - \mathbf{R})\} \times \Phi^{\mathbf{i},\mathbf{j}}_{\alpha,\beta}(\tau_{\mathbf{i}} - \tau_{\mathbf{j}} - \mathbf{R}) \quad . \tag{1}$$

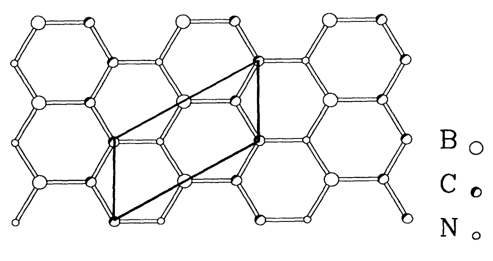

FIG. 1. Atomic structure of a hexagonal BC_2N sheet. The largest open circles denote B atoms while the smallest open circles denote N atoms. The shaded circles denote C atoms. The unit cell is denoted as a parallelogram, which is two times larger than the unit cells of graphite and BN.

0163-1829/95/52(20)/14971(5)/$06.00

Here $\Phi^{\mathbf{i},\mathbf{j}}_{\alpha,\beta}(\tau_\mathbf{i}-\tau_\mathbf{j}-\mathbf{R})$ denotes force constants and $\mathbf{R}$ denotes lattice vectors. Labels $\mathbf{i}$ and $\mathbf{j}$ denote the atoms in the unit cell, while α and β denote the Cartesian coordinates x, y, and z of the atomic displacement. Here, $\mathbf{M}_\mathbf{i}$ and $\tau_\mathbf{i}$ denote the mass and position of each atom in the unit cell, respectively. In order to calculate the force constants, supercell total-energy calculations are performed within the framework of the local-density approximation with the use of pseudopotentials and plane wave basis sets. For the nonlocal parts of the pseudopotentials, the separable form[15] is used. The force constants for each atom are calculated by considering interactions up to second neighbors, while more accurate phonon dispersions of graphite sheets have been obtained by taking up to fourth neighbors into account,[12] which shows the best fit with the data of neutron diffraction.[11] Despite some detailed differences, the features of the phonon dispersions for a graphite sheet are similar in the experimental data,[11] the previous calculations,[12] and our present calculations. Supercells consisting of eight atoms are used to calculate the force constants of graphite, BN, and BC_2N sheets. In the case of the graphite sheet, we have checked that the changes of force constants are tiny when we calculate them by using a supercell consisting of 24 atoms. This change results in minor differences in phonon dispersion curves which will not change our present conclusions. From this numerical experience, we believe that, in order to compare the phonon spectra among graphite, BN, and BC_2N sheets, it is enough to take up to the second neighbors for the force constants by using eight-atom supercells. A cutoff energy of 50 Ry for the plane wave basis sets is found to be sufficient to obtain well converged phonon frequencies. Prior to the calculations of the force constants, the equilibrium geometries are obtained by restricting the Hellmann-Feynman forces on each atom to be less than 6×10^{-3} Ry/(a.u.). The stable geometries of graphite and BN sheets are flat while the BC_2N sheet is found to be slightly distorted. Force constants for all the atoms are calculated by comparing Hellmann-Feynman forces before and after the displacement of each atom from its equilibrium position. The amount of the displacement is 0.05 a.u. for each direction along the the x, y, and z axes. The symmetry relation of the force constants

$$\Phi^{\mathbf{i},\mathbf{j}}_{\alpha,\beta}(\tau_\mathbf{i}-\tau_\mathbf{j}-\mathbf{R}) = \Phi^{\mathbf{j},\mathbf{i}}_{\beta,\alpha}(-\tau_\mathbf{i}+\tau_\mathbf{j}+\mathbf{R}) \quad (2)$$

and

$$\Phi^{\mathbf{i},\mathbf{j}}_{\alpha,\beta}[\mathbf{S}\cdot(\tau_\mathbf{i}-\tau_\mathbf{j}-\mathbf{R})] = \mathbf{S}^{\mathbf{t}}\cdot\Phi^{\mathbf{i},\mathbf{j}}_{\alpha,\beta}(\tau_\mathbf{i}-\tau_\mathbf{j}-\mathbf{R})\cdot\mathbf{S} \quad (3)$$

are found to be satisfied within an error of 10% in most components of the calculated force constants. (Here $\mathbf{S}$ denotes a matrix for symmetry operation which keeps the equilibrium geometry invariant.) This error causes an uncertainty in phonon frequencies of $\sim$30 cm^{-1} in the present calculations. The numerically obtained force constants are symmetrized according to above relations.

III. RESULTS

The calculated highest phonon frequencies at the Γ point for the graphite and BN sheets are 1555 cm^{-1} and 1299 cm^{-1}, respectively, which are reasonable when compared to the corresponding experimental data of 1600 cm^{-1} for bulk graphite[11] and 1366 cm^{-1} for bulk hexagonal BN.[16] In both cases, these phonon modes are doubly degenerate consisting of stretching and shear modes. This is because of the threefold symmetry of graphite and BN. The corresponding phonon modes at the Γ point of BC_2N split into two frequencies due to the lack of this symmetry, 1442 cm^{-1} for the stretching mode and 1394 cm^{-1} for the shear mode. This splitting would be a good indicator for frequency measurement in BC_2N, such as Raman scattering or infrared absorption.

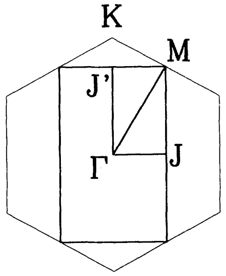

FIG. 2. The first Brillouin zone of the BC_2N sheet (inner rectangle) related to the Brillouin zone for graphite and BN sheets (outer hexagon). The vertical direction is parallel to the vertical direction of Fig. 1, i.e., parallel to C-C and B-N chains of the BC_2N sheet. The high symmetry points are also shown.

We now present results for the phonon dispersion curves. The unit cell of the BC_2N sheet is two times larger than those of the graphite and BN sheets, as can be seen in Fig. 1. Hereafter, the unit cell of the BC_2N sheet is referred to as a 2×1 unit cell, while the unit cells of graphite and BN sheets are referred to as 1×1 unit cells. Figure 2 shows the first BZ of the 2×1 unit cell relative to the 1×1 unit cells, and Fig. 3 shows the phonon dispersion curves for graphite, BN, and BC_2N sheets along the symmetry lines of the 2×1 unit cell. For the phonon dispersions of the graphite and BN sheets, the folding of the first BZ of the 1×1 unit cell into that of the 2×1 unit cell is considered. The right lower panel of Fig. 3 contains a superposition of the phonon frequencies of graphite and BN sheets for comparison with a BC_2N sheet. Despite differences in detail, the gross features of the phonon dispersion of the BC_2N sheet is similar to the superposition of those of the graphite and BN sheets. The phonon dispersions along the lines J'-M and M-J in the lower panels of Fig. 3 are easier to compare, since the phonons on these lines remain unfolded. For the acoustic modes of the BC_2N sheet, the slopes seem to be almost equal in the directions Γ-J' and Γ-J, which correspond to the directions parallel and perpendicular to C-C and B-N chains. Furthermore, the slopes in the direction of Γ-M are also the same as those before. From this result, the sound velocity in the BC_2N sheet is expected to be isotropic. The anisotropic atomic structure shown in Fig. 1 makes most of the BC_2N tubule have chiral properties. For example, chirality in the tubule conductivity was previously predicted.[7] On the other hand, the sound

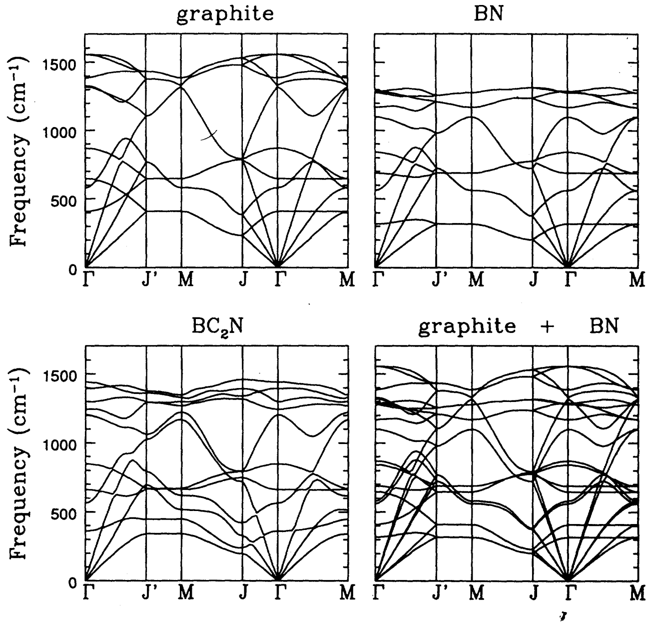

FIG. 3. Calculated phonon dispersion curves of graphite and BN sheets (upper panels) and a BC$_2$N sheet (lower left panel). For comparison, a superposition of the curves of graphite and BN is also shown in the right lower panel.

propagation along the tubule axis is expected not to have chiral properties according to the present results.

Despite a difference in symmetry properties among these sheets, phonon modes of the BC$_2$N sheet at the Γ point are similar to those of the graphite and the BN sheets at the Γ and M points because of the zone folding. Away from the Γ points, the phonon modes of BC$_2$N can still be related to those of graphite and BN sheets. Here we illustrate particular phonon modes of the BN and BC$_2$N sheets at the K point of the 1×1 unit cell. (The corresponding point for the 2×1 unit cell is located two thirds of the way from the Γ point toward the J' point of Fig. 2.) Figures 4 and 5 show phonon modes of the BN and BC$_2$N sheets, respectively. Corresponding phonon frequencies lie in the same range, 1144 cm^{-1} and 1014 cm^{-1} for the BN sheet, and 1179 cm^{-1} and 1114 cm^{-1} for the BC$_2$N sheet. The direction of the arrows in Figs. 4 and 5 denotes the direction of the atomic displacement, while lengths are magnified compared to the atomic replacement. For the BN sheet, the phonon of higher frequency is dominated by B vibration while the phonon of lower frequency is dominated by N vibration. This result is consistent with the heavier mass of the N atom. Even with the atomic displacements, the system still has threefold symmetry around the static sites.[17]

For the BC$_2$N sheet, the phonon of higher frequency is dominated by B and C vibrations while the phonon of lower frequency is dominated by C and N vibrations as shown in Fig. 5. This is also consistent with the heavier reduced mass for the phonon of lower frequency. An interesting point is that the system appears to have threefold symmetry if we ignore the minor differences in

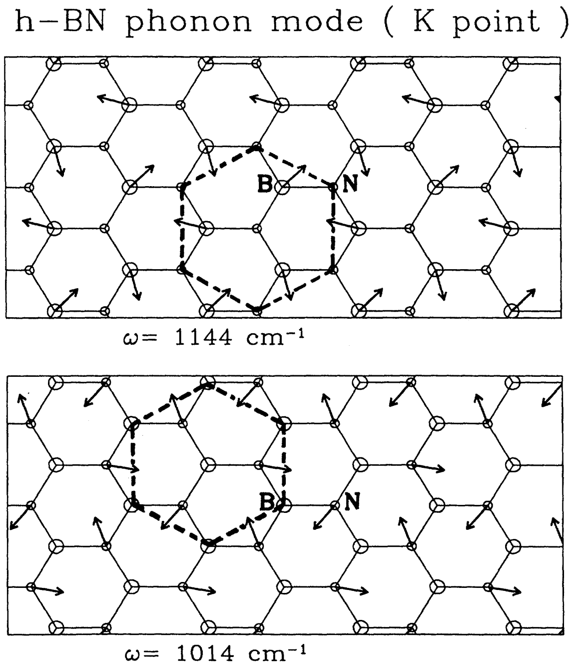

FIG. 4. Snapshot for atomic motions in the BN sheet associated with phonons at the K point with frequencies of 1144 cm^{-1} (top) and 1013 cm^{-1} (bottom). Arrows indicate the directions of atomic displacements from the equilibrium positions. The larger hexagons drawn with thick broken lines denote irreducible units of the atomic displacement. The directions of the arrows change for a snapshot at a different time.

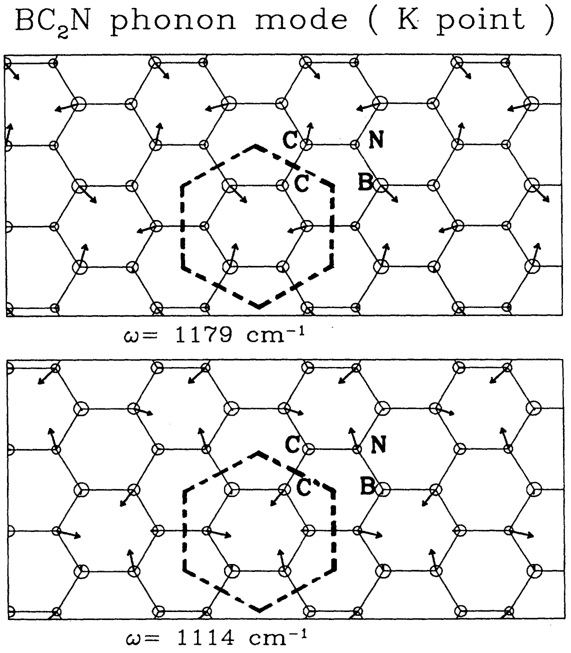

FIG. 5. Snapshot for atomic motions in the BC$_2$N sheet associated with phonons at the K point with frequencies of 1179 cm^{-1} (top) and 1114 cm^{-1} (bottom). As in the case of Fig. 4, the larger hexagons of thick broken lines denote the irreducible units and the directions of the arrows will be changed at a different time.

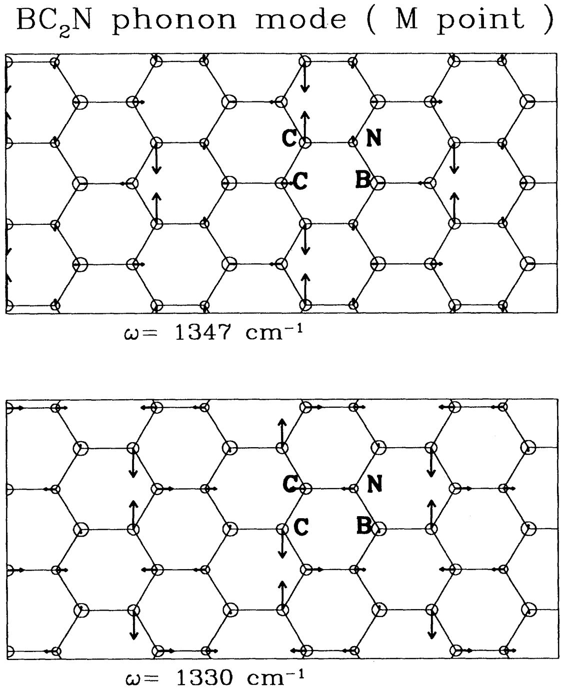

FIG. 6. Snapshot for atomic motions in the BC_2N sheet associated with phonons at the M point with frequencies of 1347 cm^{-1} (top) and 1330 cm^{-1} (bottom).

the magnitude of atomic displacements. The obvious difference in this case is that the symmetry center here is the center of each hexagon. (Of course, this displacement does not exactly have threefold symmetry since the original structure of the BC_2N sheet lacks this symmetry.) In the graphite sheet, the corresponding modes also exist. The center of the threefold symmetry is either the atomic site or the center of each hexagon depending on the frequencies. Even though the symmetry property of the general phonon modes of the BC_2N sheet is different from those of graphite and BN sheets, the geometric features have relationships similar to the case which we have illustrated above. However, in sharp contrast, unique phonon modes of the BC_2N sheet are found to appear at wave vectors along the J'-M line of Fig. 2. The corresponding figures of the atomic displacements are shown in Fig. 6 associated with the phonon at the M point with frequencies of 1347 cm^{-1} and 1330 cm^{-1}. In these vibrational modes, the coexistence of the displaced atoms into two orthogonal directions, i.e., parallel and perpendicular to C-C and B-N chains of the BC_2N sheet, is always observed, while such a mode is not seen for the cases of the graphite and BN sheets.

The calculated phonons of the BC_2N sheet show negligible coupling between in-plane and out-of-plane modes. Meanwhile, the coupling will increase when the sheets bend, so phonons of small diameter tubules of these sheets should have different features. On the other hand, phonons of rather large diameter tubules are simply obtained by the same zone-folding technique as in the case of band structure calculations.[10] The phonon frequencies of graphitic sheets thus are also useful for identifying the composition and structure of tubules by measuring vibrational frequencies.

Finally, we comment on the conductivity of the BC_2N tubules arising from electron-phonon scattering in the sheet. The BC_2N sheet and tubules are semiconductors so these have to be doped with either donors or acceptors to obtain higher conductivity.[7] In both doping cases, the wave function of the carriers is found to be concentrated only on C sites according to our recent calculations.[18] This result raises an interesting question as to whether the electron-phonon coupling in a BC_2N sheet is larger than that in a graphite sheet. Recently, Jishi, Dresselhaus, and Dresselhaus[14] estimated the relaxation time of the carrier in carbon nanotubes to be almost 50 times longer than that in copper. If the relaxation time of the BC_2N tubule is of comparable size, a remarkably large current is expected for BC_2N tubules. This current may generate measurable magnetic fields since the BC_2N tubule is expected to have chiral conductivity.[7]

IV. CONCLUDING REMARKS

In summary, we have calculated the phonon spectra of graphitic sheets of carbon, BN, and BC_2N within the harmonic approximation using force constants determined by *ab initio* supercell calculations. The calculated phonon dispersions of the BC_2N sheet can be expressed approximately as a superposition of those of graphite and BN sheets. The similarities and differences in the geometric displacements of the phonon modes among these graphitic sheets depend on the wave vector of the phonons. The present results should be useful in identifying graphitic compounds by measuring vibrational frequencies and also useful in performing further investigation of electron-phonon coupling in these systems.

ACKNOWLEDGMENTS

This work was supported by National Science Foundation Grant No. DMR91-20269 and by the Director, Office of Energy Research, Office of Basic Energy Sciences, Materials Sciences Division of the U.S. Department of Energy under Contact No. DE-AC03-76SF00098. Part of the present calculations were done using the CRAY-C90 computer at the San Diego Supercomputer Center. Y.M. acknowledges support from the Fundamental Research Laboratories of NEC Corporation.

---

[*] Permanent address: Fundamental Research Laboratories, NEC Corporation, 34 Miyukigaoka, Tsukuba 305, Japan.

[1] K.M. Krishnan, Appl. Phys. Lett. **58**, 1857 (1991).

[2] J. Kouvetakis, T. Sasaki, C. Shen, R. Hagiwara, M. Lerner, K.M. Krishnan, and N. Bartlett, Synth. Met. **34**, 1 (1989).

[3] X. Blase, A. Rubio, S.G. Louie, and M.L. Cohen, Phys. Rev. B **51**, 6868 (1994).

[4] R.M. Wentzcovitch, M.L. Cohen, S.G. Louie, and D.

Tománek, Solid State Commun. **67**, 515 (1988); D. Tománek, R.M. Wentzcovitch, S.G. Louie, and M.L. Cohen, Phys. Rev. B **37**, 3134 (1988).

[5] A.Y. Liu, R.M. Wentzcovitch, and M.L. Cohen, Phys. Rev. B **39**, 1760 (1988).

[6] A. Rubio, J.L. Corkill, and M.L. Cohen, Phys. Rev. B **49**, 5081 (1994); X. Blase, A. Rubio, S.G. Louie, and M.L. Cohen, Europhys. Lett. **28**, 335 (1994).

[7] Y. Miyamoto, A. Rubio, M.L. Cohen, and S.G. Louie, Phys. Rev. B **50**, 4976 (1994); Y. Miyamoto, A. Rubio, S.G. Louie, and M.L. Cohen, *ibid.* **50**, 18 360 (1994).

[8] S. Iijima, Nature **354**, 56 (1991).

[9] O. Stephan, P.M. Ajayan, C. Colliex, Ph. Redlich, J.M. Lambert, P. Bernier, and P. Lefin, Science **266**, 1683 (1994); Z. Weng-Sieh, K. Cherrey, N.G. Chopra, X. Blase, Y. Miyamoto, A. Rubio, M.L. Cohen, S.G. Louie, A. Zettl, and R. Gronsky, Phys. Rev. B **51**, 11 229 (1995).

[10] N. Hamada, S. Sawada, and A. Oshiyama, Phys. Rev. Lett. **68**, 1579 (1992); M.S. Dresselhaus, G. Dresselhaus, and R. Saito, Solid State Commun. **84**, 201 (1992).

[11] See, for example, C. Oshima, T. Aizawa, R. Souda, Y. Ishizawa, and Y. Sumiyoshi, Solid State Commun. **65**, 1601 (1988).

[12] See, for example, R. Al-Jishi and G. Dresselhaus, Phys. Rev. B **26**, 4514 (1982).

[13] L. Pietronero, S. Strässler, and H.R. Zeller, Phys. Rev. B **22**, 904 (1980).

[14] R.A. Jishi, M.S. Dresselhaus, and G. Dresselhaus, Phys. Rev. B **48**, 11 385 (1993).

[15] L. Kleinman and D.M. Bylander, Phys. Rev. Lett. **48**, 1425 (1982).

[16] R.J. Nemanich, S.A. Solin, and R.M. Martin, Phys. Rev. B **23**, 6348 (1981).

[17] The BN sheet has another mode having threefold symmetry with frequency of 1252 cm^{-1}. In this case, the center of symmetry is the center of each hexagon and all atoms are moving.

[18] Y. Miyamoto, S.G. Louie, and M.L. Cohen (unpublished).